Emirates Journal for Engineering Research

Volume 25 | Issue 3 Article 1

5-11-2020

Analysis and Design of a Soft Switching Z-Source Boost DC-DC Converter

Mahdi Rezvanyvardom
m-rezvanyvardom@araku.ac.ir

Amin Mirzaei
Arak University, a-mirzaee@araku.ac.ir

ANALYSIS AND DESIGN OF A SOFT SWITCHING Z-SOURCE BOOST DC-DC CONVERTER

Mahdi Rezvanyvardom[1], Amin Mirzaei[2]

[1]*Assistant Professor, Department of Electrical Engineering, Faculty of Engineering, Arak University, Arak, Iran, email m-rezvanyvardom@araku.ac.ir*

[2] *Assistant Professor, Department of Electrical Engineering, Faculty of Engineering, Arak University, Arak, Iran, email a-mirzaee@araku.ac.ir*

(Received 1st February and Accepted 11th May 2020)

تحليل وتصميم مصدر مقاومة DC–DC محول مع تقنية التبديل لينة

ملخص

تقترح هذه الورقة محول مصدر مقاومة DC–DC بتبديل مرتفع ومحول إلى حد كبير ، والذي يستخدم مسارين للرنين لإنشاء ظروف تحويل ناعمة للمفاتيح والثنائيات ويزيد أيضًا من زيادة الجهد. يحتوي المحول المقترح على مفتاح واحد فقط ، لذلك يحتوي على بنية بسيطة. علاوة على ذلك ، فإن دائرة التحكم الخاصة بها تظل تعديل عرض النبض. نظرًا لتوفير ظروف التبديل الرخوة لجميع عناصر التبديل ، فإن كفاءة المحول عالية جدًا. هذا المحول لديه أيضا جميع مزايا المحولات Z– المصدر . يتم تحليل المحاكاة ومحاكاة في برنامج PSPICE. تؤكد النتائج المزايا والميزات المذكورة أعلاه للمحول المقترح.

Abstract

This paper proposes a high step-up fully soft switched Z-source Boost DC-DC converter, which uses two resonant paths to create soft switching conditions for switches and diodes and also increases the voltage gain. The proposed converter only has one switch, so it has a simple structure. Furthermore, its control circuit remains pulse width modulation. Since soft switching conditions are provided for all switching elements, the converter efficiency is very high. This converter also has all advantages of Z-source converters. The converter is analyzed and simulated in PSPICE software. The results confirm the aforementioned advantages and features of the proposed converter.

1. INTRODUCTION

In recent years, the use of switching power supplies has become widespread in the industries. Therefore, the presentation of new topologies for DC-DC switching converters has been considered to improve the performance of these resources [1-4]. Switching converters are divided into three general categories of voltage-source converters, current-source converters and impedance-source (Z-source) converters. Unfortunately, most of the renewable-energy sources such as; solar cells have low and variable output voltages. As a result, using high step-up DC-DC converters can increase their output voltage and stabilize it [5-8]. The Block diagram of a grid-connected standalone PV system is presented in Figure 1. Due to the low output voltage of solar panels, the step-up DC-DC converter is one of the most important parts in the PV system as shown in Figure 1. One of the main advantages of the Z-source converters in comparison with the voltage-source and current source-converters is the higher voltage gain, which allows the designers to use fewer transformers in their topologies [9, 10]. Nowadays, reducing the volume and weight of switching power supplies is very important in designing. Therefore, high switching frequency is used to implement the power supplies. However, the use of high switching frequencies can increase the switching losses and also reduce the efficiency of the circuit. Thus, soft switching techniques are applied to solve these problems. On the other hand, the use of them is a good way to reduce radio-frequency interference (RFI) and electromagnetic interference (EMI) [11-18]. In today's modern converters; the Z-source structures are highly considered for their advantages, such as high-voltage gain, clamped switch voltage, and higher reliability versus load variations [19, 20]. Z-source converter that was first suggested by Peng in 2003 [21]. Recently, lots of topologies based on Z-source converter have been proposed by researchers to improve the voltage gain. Although, most of them have lots of elements, high complexity, high volume and low efficiency [22-

30]. The proposed topologies in [23, 25] use transformer to create isolation between input and output. Conduction and switching losses are high due to use the transformer and hard switching condition. Low switching frequency and high number of passive elements in [27] leads to high volume and weight for the converter. Furthermore, its efficiency is low due to hard switching condition. The proposed converters in [24, 26] have complex structure and control. Besides they suffer from hard switching condition.

In this paper, a Boost Z-source DC-DC converter is proposed that uses soft switching techniques (ZCS and ZVS) for the main switch and diodes. The proposed converter is a Z-source converter that uses the impedance source network and two resonant paths to increase the voltage gain. The converter has simple structure due to use of one power switch. Moreover, pulse width modulation (PWM) control is applied to trigger the switch. The operation modes of the proposed converter, theoretical waveform and simulation results are explained. Finally, the conclusions are presented in the last section.

2. OPERATING PRINCIPLES OF THE PROPOSED CONVERTER

Figure 2 shows the structure of the proposed converter. It is used only one switch (S_1) in the topology. Besides, L_1 is the input filter inductor.

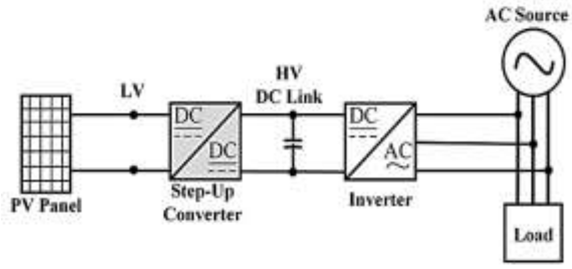

Figure1. The Block diagram of a grid-connected standalone PV system

The inductances of L_{q1} and L_{q2} are equal, and they are the main inductors of Z-source structure. These inductors are coupled with series inductors in the resonance paths (L_{S1} and L_{S2}), respectively. The capacitances of C_1 and C_2 are equal, and they are the main capacitors of Z-source structure. These capacitors have high values, and the voltages across them are constant and equal. Consequently, they can be replaced with DC sources. Capacitor C_3 is connected in parallel with the switch and has small value. C_4 and C_5 are resonant capacitors that are used to provide soft switching conditions and to increase the voltage gain. In addition, L_{LK1} and L_{LK2} are resonant inductors. D_1 and D_2 are diodes that are placed in the resonant paths. Furthermore, D_o is an output diode that provides power transmission from the input to the output. Moreover, C_o is the output capacitor. Inductor L_2 also controls the current that flows to switch S_1. The theoretical waveforms for the proposed converter is depicted in Figure 3. This converter has all advantages of Z-source converter, which include:

- Higher voltage gain for the same duty cycle.
- Lower inrush current.
- Higher reliability (separation of load and source from each other in case of short circuit at the load side).
- Lower Harmonic injection.
- Second-order output filter [31].

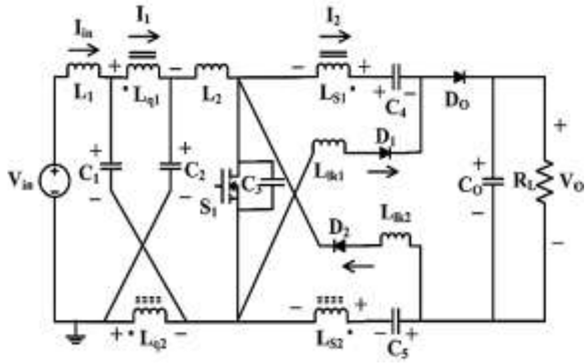

Figure 2. The proposed Z-source Boost DC-DC converter

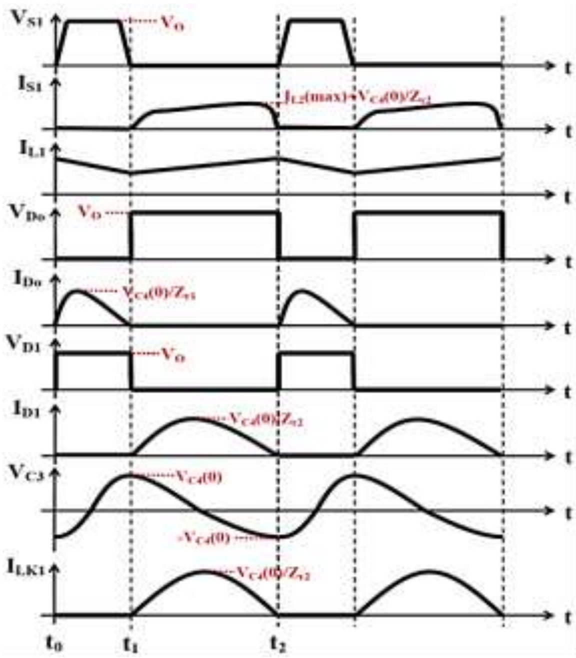

Figure 3. The theoretical waveforms for the proposed converter

In each switching cycle, the proposed converter has two modes of operation, which will be discussed below.

Mode 1 ($t_0<t<t_1$): During this mode, switch S_1 is turned off, while output diode D_o is forward biased to transfer the power from the input to the output. Furthermore, a resonance between capacitors C_4 and C_5 and inductors L_2, L_{S1} and L_{S2} occurs. Therefore,

the inductor currents are decreased, and the capacitor voltages are increased. If the initial voltages of the capacitors C_4 and C_5 are equal to -V_{C4} (0), then the following equation is obtained.

$$V_{C4}(t) = V_{C5}(t) = -V_{C4}(0)\cos\omega_{r1}(t - t_0) \qquad 1$$

Since the circuit has symmetric structure, then $C_1 = C_2$, $L_{q1} = L_{q2} = L_q$, $L_{S1} = L_{S2} = L_S$, $C_4 = C_5$, $L_{Lk1} = L_{Lk2} = L_{Lk}$. As a result, the following equation is obtained.

$$C_{eq1} = \frac{C_2}{2} \qquad L_{eq1} = 2L_S + L_2 \qquad 2$$

$$\omega_{r1} = \frac{1}{\sqrt{C_{eq1}L_{eq1}}} \qquad Z_{r1} = \sqrt{\frac{L_{eq1}}{C_{eq1}}} \qquad 3$$

$$i_{L2}(t) = i_{LS}(t) = -\frac{V_{C4}(0)}{Z_{r1}}\sin\omega_{r1}(t - t_0) \qquad 4$$

The voltage across capacitors C_1 and C_2 are always constant, and these capacitors can be assumed like a DC voltage source. Moreover, the current flows through input filter inductor L_1 is constant and is equivalent to a DC current source. During this mode, diodes D_1 and D_2 are reverse biased and the current that flows through resonant inductors L_{Lk1} and L_{Lk2} is zero.

$$L_{eq} = n^2L_S \qquad 5$$

$$I_{C1} = I_{C2} \rightarrow I_{in} = 2I_{C1} + I_2 = 2I_{C1} + \frac{I_1}{n} \qquad 6$$

Capacitor C_3 is very small. Thus at the beginning of this mode, it is charged in a short time and the voltage across it will be equal to V_o. Therefore, no current flows through the capacitor during this mode. This mode ends when the voltage across capacitors C_4 and C_5 reaches to its maximum value (V_{C4} (0)) and the current that flows through inductors L_2, L_{S1} and L_{S2} reaches zero. At the end of this mode, output diode D_o is turned off under ZCS condition. The duration of this mode is determined as follows. The equivalent circuit for mode 1 is depicted in Figure 4.

$$t_1 - t_0 = \frac{1}{2f_{r1}} \qquad 7$$

Mode 2 (t_1<t<t_2): This mode starts when switch S_1 is turned on at t_1. It is turned on under ZCS condition because the currents flow through inductors L_2, L_{S1}, and L_{S2} are zero. When switch S_1 is turned on, two resonant paths are created. The first resonance starts between capacitor C_4 and inductors L_{S1} and L_{LK1} through diode D_1 and switch S_1. Therefore, diode D_1 is turned on under ZCS condition. This is done because the diode is connected in series with inductor L_{Lk1}, which has zero current at t_1.
Similarly, the second resonance starts between capacitor C_5 and inductors L_{S2} and L_{Lk2} through diode D_2 and switch S_1. Consequently, diode D_2 is turned on under ZCS condition. This phenomena occurs because the diode is connected in series with Furthermore, the currents of inductors L_{Lk1} and L_{Lk2} are increased sinusoidally.

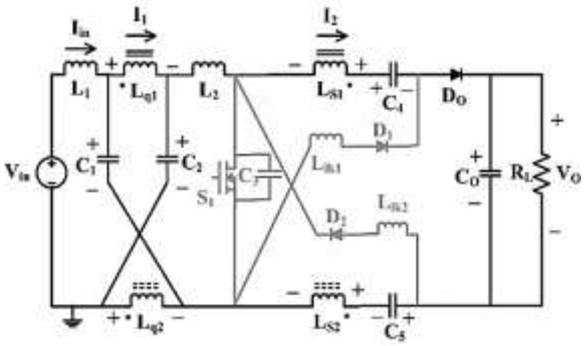

Figure 4. The equivalent circuit for mode 1

$$L_{eq2} = L_{Lk1} + L_{S1} \qquad 8$$

$$\omega_{r2} = \frac{1}{\sqrt{C_4L_{eq2}}} \qquad Z_{r2} = \sqrt{\frac{L_{eq2}}{C_4}} \qquad 9$$

$$V_{C4}(t) = V_{C5}(t) = V_{C4}(0)\cos\omega_{r2}(t - t_1) \qquad 10$$

$$i_{LS}(t) = i_{Lk}(t) = \frac{V_{C4}(0)}{Z_{r2}}\sin\omega_{r2}(t - t_1) \qquad 11$$

$$I_{Lk} = I_{Lk1} = I_{Lk2} \rightarrow I_{S1} = I_{L2} + 2I_{Lk} \qquad 12$$

During this mode, output capacitor C_O supplies the load, while output diode D_o is reverse biased. This mode ends when the voltage across capacitors C_4 and C_5 reaches -V_{C4} (0), while the resonance currents that flow through inductors L_{S1}, L_{S2}, L_{Lk1} and L_{Lk2} are zero.

$$t_2 - t_1 = \frac{1}{2f_{r2}} \qquad 13$$

Since switch S_1 is turned on, the voltage across capacitor C_3, which is connected in parallel with the switch is zero during this mode. As a result, at the end of this mode, switch S_1 can be turned off under ZVS condition. The equivalent circuit for mode 2 is depicted in Figure 5.

3. SIMULATION RESULTS

A 120W of the proposed Z-source Boost DC-DC converter is designed and simulated. The input voltage of the converter is 48 volts, and its output voltage is 384 volts.

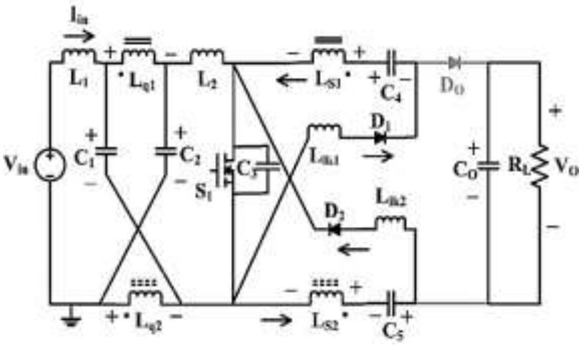

Figure 5. The equivalent circuit for mode 2

The switching frequency is 100 kHz for the switch. The type of diodes and switch are selected based on the voltage and current stresses [32]. Circuit parameters with details including type of materials and their values based on the design considerations are presented in Table 1.

Figure 6(a) shows the voltage and current waveforms of switch S_1 and their zoom versions are depicted in Figure 6(b). According to the converter operation, switch S_1 is turned on under ZCS condition. This is done because the current flows through inductors L_2, L_{S1} and L_{S2} is zero. Based on the converter operation in mode 2, switch S_1 is turned off under ZVS condition. This phenomena occurs because the voltage across capacitor C_3 that is connected in parallel with the switch is zero. Figure 7(a) shows input filter inductor current I_{L1} waveform, which has a low ripple and indicates the converter operation in the CCM mode. Furthermore, Figure 7(b) shows the voltages across capacitors C_1 and C_2, which have constant values. Figure 8(a) shows inductor current I_{L2} waveform. The voltage across resonant capacitors ($V_{C3} = V_{C4}$) is shown in Figure 8(b), which is sinusoidal due to the resonance operation of the converter and varies between V_{C4} (0) and $-V_{C4}$ (0). The values of the input and output voltages are shown in Figure 9(a). Moreover, resonant inductors currents $I_{Lk1} = I_{Lk2}$ waveforms are shown in Figure 9(b), which are sinusoidal due to the converter operation. The voltage across capacitor C_3 is similar to the voltage across switch S_1. Figure 10(a) shows the voltage and current waveforms for diodes D_1 and D_2, which are similar to each other. Besides, their zoom versions are depicted in Figure 10(b).

Table 1-Parameters of the proposed converter

PARAMETERS	TYPE	VALUE
Power Switch (S_1)	IRF120	-
Diodes (D_1, D_2, D_o)	UF4004	-
Inductor (L_2)	-	100 μH
Resonant Inductors (L_{Lk1}, L_{Lk2})	-	30 μH
Coupled Inductors	-	-
(L_{S1}, L_{S2})	-	0.4 μH
(L_{q1}, L_{q2})	-	10 μH
Turn Ratio	-	5
Input Filter Inductor (L_1)	-	200 μH
Capacitors (C_1, C_2)	-	100 μF
Resonant Capacitors (C_4, C_5)	-	90 nF
Capacitor (C_3)	-	2 nF
Output Capacitor (C_o)	-	100 μF

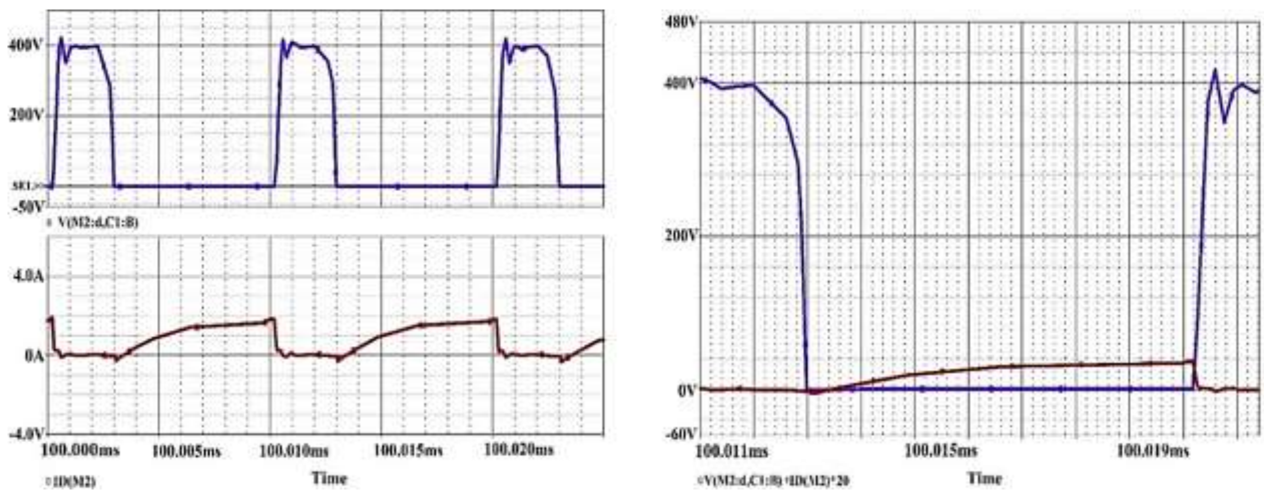

(a) (b)

Figure 6. (a) The voltage and current waveforms of switch S_1, (b) zoom version

Based on the converter operation in mode 2, these diodes are turned on simultaneously under ZCS condition. This is due to series connections of resonant inductors L_{Lk1} with diode D_1 and L_{Lk2} with diode D_2, which has zero current when switch S1 is turned on. Moreover, the diodes are also turned off under ZCS condition. Figure 11(a) shows the voltage and current waveforms of output diode D_o. Furthermore, their zoom versions are depicted in Figure 11(b).

Due to resonance between inductors L_2, L_{S1}, and L_{S2} and capacitors C_4 and C_5, the current that flows through them reaches zero at t_1. As a result, diode D_o is turned off under ZCS condition. Furthermore, diode D_o is turned on when switch S_1 turns off. The diode is turned on under ZCS condition because the current that flows through inductors L_2, L_{S1}, and L_{S2} that are connected in series with diode D_o reaches to zero again. Consequently, the power is transferred from the input to the output. The comparison of proposed ZS DC-DC converter with other similar topologies are also presented in Table 2. Due to the operation of the auxiliary cell to create soft switching conditions for all semiconductor devices, the efficiency curve for the proposed Z-source Boost DC-DC converter versus conventional Z-source converter is depicted in Figure 12. As shown in this figure, the efficiency of the proposed converter at nominal power (120 watts) is 96%, which indicates the good performance and a significant reduction of losses in the proposed converter.

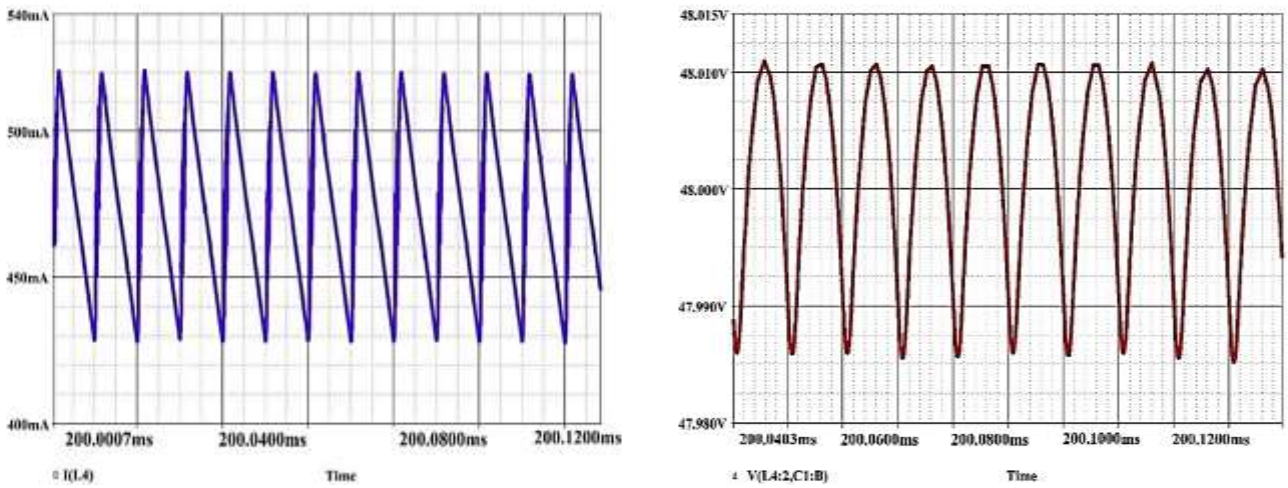

(a) (b)

Figure 7. (a) Input filter inductor current I_{L1} waveform and (b) Voltages across capacitors C_1 and C_2

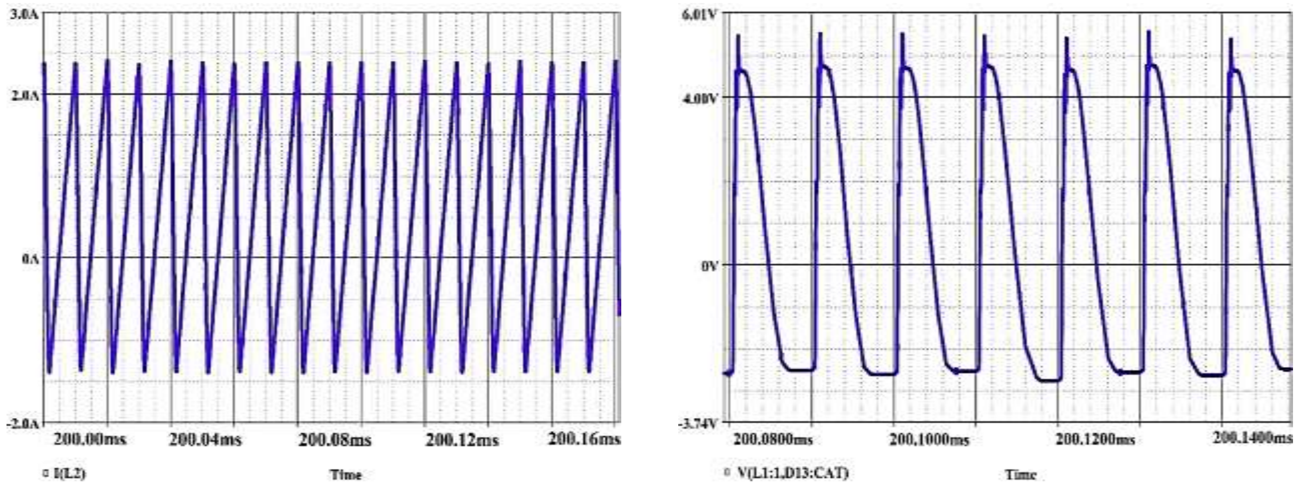

(a) (b)

Figure 8. (a) Inductor current I_{L2} waveform and (b) Voltage across resonant capacitors ($V_{C3} = V_{C4}$)

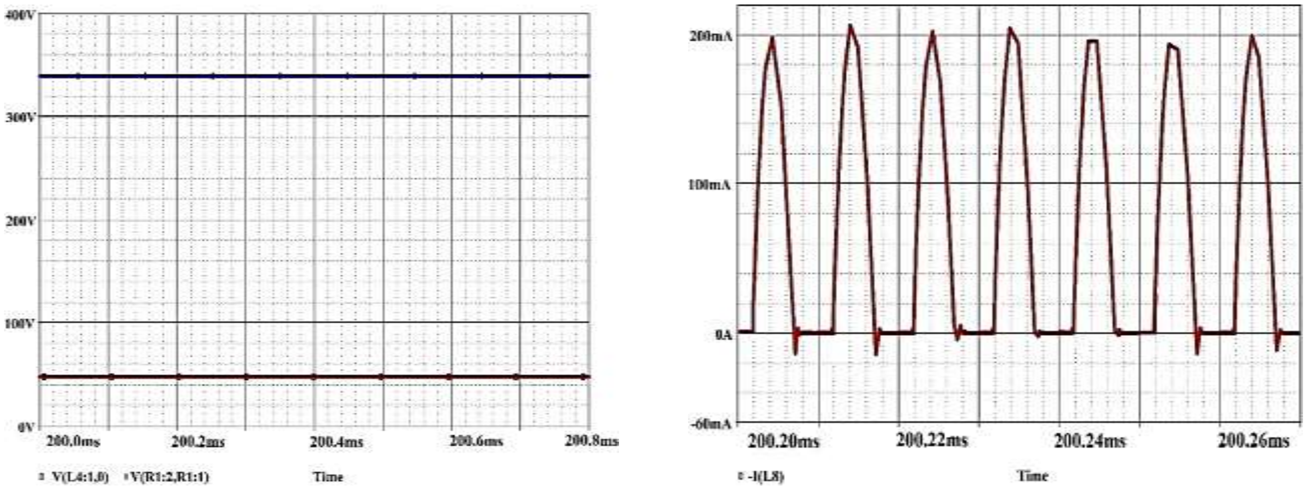

(a) (b)

Figure 9. (a) Values of the input and output voltages and (b) Resonant inductors currents $I_{Lk1} = I_{Lk2}$ waveforms

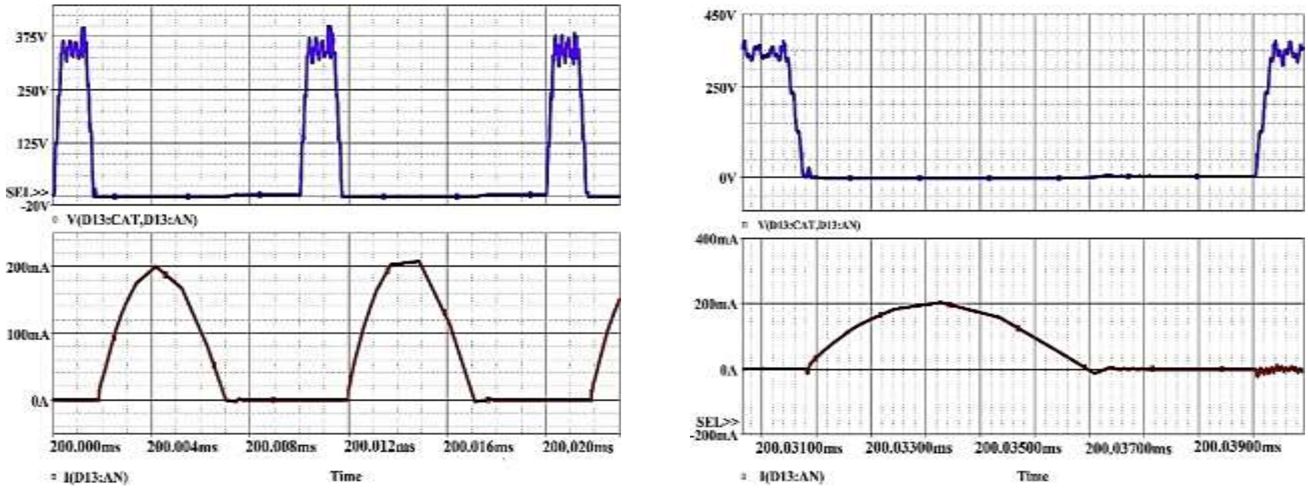

(a) (b)

Figure 10. (a) Voltage and current waveforms for diodes D_1 and D_2, (b) zoom version

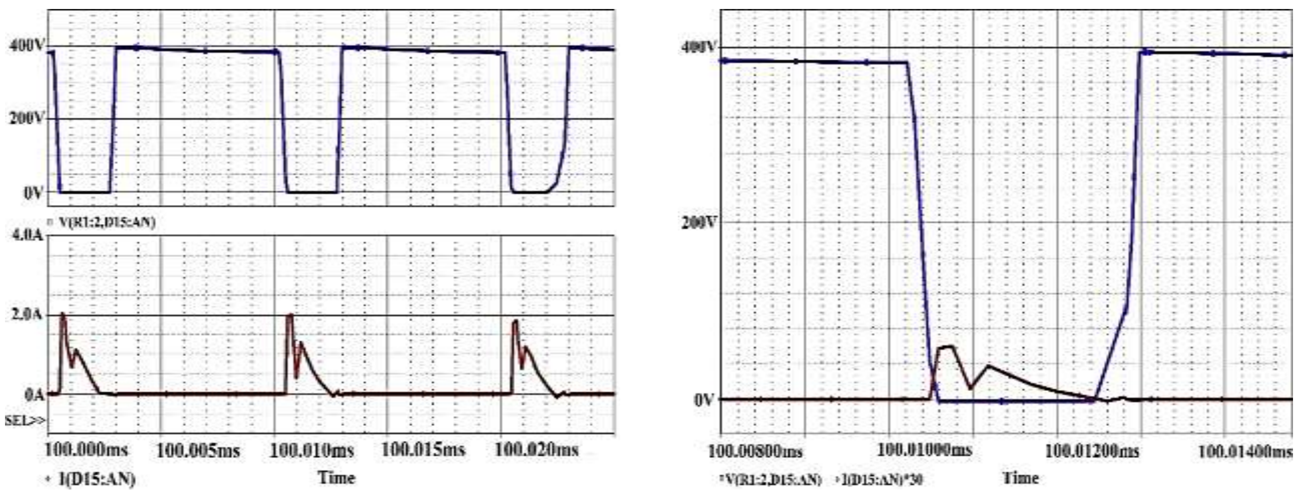

(a) (b)

Figure 11. (a) Voltage and current waveforms of output diode D_o, (b) zoom version

Table 2. The comparison between proposed ZS DC-DC converter and other similar topologies

	Ref [23]	**Ref [24]**	**Ref [25]**	**Ref [26]**	**Ref [27]**	**Proposed converter**
Voltage gain	16	10	15	15.2	7.8	8
Isolation between input and output	Yes	No	Yes	No	No	No
Input current	Continuous	Continuous	Discontinuous	Continuous	Continuous	Continuous
Components	4 Diodes 1 Switch 3 Inductors 5 Capacitors	4 Diodes 1 Switch 4 Inductors 6 Capacitors	2 Diodes 1 Switch 2 Inductors 3 Capacitors	5 Diodes 1 Switch 3 Inductors 7 Capacitors	6 Diodes 2 Switches 2 Inductors 2 Capacitors	2 Diodes 1 Switch 8 Inductors 5 Capacitors
Output power	300 W	100 W	500 W	150 W	3 KW	120 W
Switching voltage stress	$\frac{V_O}{n(1+D)}$	$\frac{V_{in}}{1-4D}$	$\frac{V_{in}}{1-2D}$	$\frac{V_{in}}{1-2D}$	$\frac{1+D}{1-3D}V_{in}$	$\frac{V_{in}}{1-2D}$
Soft switching condition	No	No	No	No	No	Yes
Switching frequency	50 KHz	30 KHz	10 KHz	40 KHz	5 KHz	100 KHz

4. CONCLUSION

This paper proposes a high step-up fully soft switched Z-source Boost DC-DC converter, which uses two resonant paths to create soft switching conditions for semiconductor devices and also increases the voltage gain in the circuit. The proposed converter only has one switch, so it has a simple structure. Furthermore, its control circuit remains pulse width modulation (PWM). Therefore, the proposed converter has much less complexity compared to similar structures. Besides, the proposed converter uses the impedance network structure in the main power path from the input to the output.

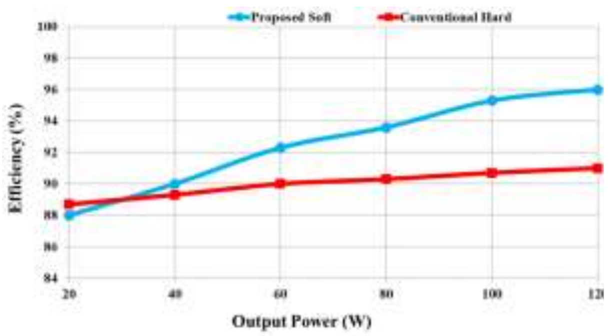

Figure 12. Efficiency curve of the proposed converter versus conventional Z-source converter

As a result, the current rate of the circuit element is very low. Since the soft switching conditions are provided for semiconductor devices, the converter efficiency is very high. A 120W of the converter operating at 100 kHz is simulated by PSPICE software. Furthermore, to verify the proposed converter performance, voltage conversion of 48 V/384 V is provided. The voltage gain of the proposed converter is eight without using transformer in its structure. The measured efficiency of the proposed Z-source Boost converter is 96% at full load which is around 6% higher than conventional Z-source converter.

REFERENCES

1. A. Mirzaei, A. Jusoh, Z. Salam, E. Adib and H. Farzanehfard, "Analysis and design of a high efficiency bidirectional DC–DC converter for battery and ultracapacitor applications," Simulation Modelling Practice and Theory, vol. 19, pp. 1651-1667, 2011.
2. A. Ganjavi, H. Ghoreishy and A. A. Ahmad, "A Novel Single-Input Dual-Output Three-Level DC–DC Converter," in IEEE Transactions on Industrial Electronics, vol. 65, no. 10, pp. 8101-8111, 2018.
3. Y. Cao, V. Samavatian, K. Kaskani and H. Eshraghi, "A Novel Nonisolated Ultra-High-Voltage-Gain DC–DC Converter With Low Voltage Stress," in IEEE Transactions on Industrial Electronics, vol. 64, no. 4, pp. 2809-2819, 2017.
4. A. Mirzaei, A. Jusoh and Z. Salam, “Design and implementation of high efficiency non-isolated bidirectional zero voltage transition pulse width modulated DC-DC converters," Energy Journal, vol. 47, pp. 358-369, 2012.
5. M. Forouzesh, Y. Shen, K. Yari, Y. P. Siwakoti and F. Blaabjerg, "High-Efficiency High Step-Up DC–DC Converter With Dual Coupled Inductors for Grid-Connected Photovoltaic Systems," in IEEE Transactions on Power Electronics, vol. 33, no. 7, pp. 5967-5982, 2018.
6. A. Ghosh and S. S. Saran, "High gain DC-DC step-up converter with multilevel output voltage," 2018 International Symposium on Devices, Circuits and Systems (ISDCS), Howrah, 2018, pp. 1-6.
7. L. Schmitz, D. C. Martins and R. F. Coelho, "Conception of high step-up DC-DC boost-based converters," 2017 Brazilian Power

Electronics Conference (COBEP), Juiz de Fora, 2017, pp. 1-6.
8. L. Schmitz, R. F. Coelho and D. C. Martins, "High step-up high efficiency dc-dc converter for module-integrated photovoltaic applications," 2015 IEEE 13th Brazilian Power Electronics Conference and 1st Southern Power Electronics Conference (COBEP/SPEC), Fortaleza, 2015, pp. 1-6.
9. A. Torkan and M. Ehsani, "A Novel Non isolated Z-Source DC–DC Converter for Photovoltaic Applications," in IEEE Transactions on Industry Applications, vol. 54, no. 5, pp. 4574-4583, 2018.
10. S. Hanyun , Z. Bo and Qiu, Dongyuan "Hybrid Z-source boost DC–DC converters," IEEE Transactions on Industrial Electronics, vol. 64, no. 1,pp. 310-319, 2017.
11. M. Rezvanyvardom, E. Adib and H. Farzanehfard, "Zero-current transition interleaved boost converter," 2011 2nd Power Electronics, Drive Systems and Technologies Conference, Tehran, 2011, pp. 87-91. Springer Science & Business Media.
12. A. Mirzaei, M. Rezvanyvardom, M. Taati, "High Step-up Fully Soft Switched Interleaved Sheppard-Taylor Converter with Only One Auxiliary Switch for PV Application," Solar Energy, vol. 177, pp. 455-463, 2019.
13. H. Tarzamni, E. Babaei and A. Z. Gharehkoushan, "A Full Soft-Switching ZVZCS Flyback Converter Using an Active Auxiliary Cell," in IEEE Transactions on Industrial Electronics, vol. 64, no. 2, pp. 1123-1129, 2017.
14. M. Rezvanyvardom, E. Adib and H. Farzanehfard, "A new interleaved ZCS PWM boost converter," 2010 IEEE International Conference on Power and Energy, Kuala Lumpur, 2010, pp. 45-50.
15. M. Rezvanyvardom, E. Adib, H. Farzanehfard and M. Mohammadi, "Analysis, design and implementation of zero-current transition interleaved boost converter," in IET Power Electronics, vol. 5, no. 9, pp. 1804-1812, November 2012.
16. M. Rezvanyvardom, E. Adib and H. Farzanehfard, "New interleaved zero-current switching pulse-width modulation boost converter with one auxiliary switch," in IET Power Electronics, vol. 4, no. 9, pp. 979-983, November 2011.
17. S. Rahimi, M. Rezvanyvardom and A. Mirzaei, "A Fully Soft-Switched Bidirectional DC–DC Converter With Only One Auxiliary Switch," in IEEE Transactions on Industrial Electronics, vol. 66, no. 8, pp. 5939-5947, Aug. 2019.
18. M. Rezvanyvardom and A. Mirzaei and S. Rahimi "A New Interleaved Fully Soft Switched Pulse Width Modulation Boost Converter with One Auxiliary Switch," in IET Power Electronics, Early Access, January 2019.
19. G. Chen, Y. Deng, L. Chen, Y. Hu, L .Jiang, X. He, and Y. Wang, "A Family of Zero-Voltage-Switching Magnetic Coupling Non-isolated Bidirectional DC-DC Converters," IEEE Transactions On Industrial Electronics, vol. 64, no. 8, pp. 6223 – 6233, 2017.
20. V. P. Galigekere and M. K. Kazimierczuk, "Analysis of PWM Z-Source DC-DC Converter in CCM for Steady State," IEEE Transactions On Industrial Electronics, vol. 59, no. 4, pp. 854-863, 2012.
21. F. Z. Peng, "Z-source inverter," IEEE Transactions On Industrial Applications, vol. 39, no. 2, pp. 504–510, 2003.
22. P. Behzad ,T. Arash and A. Ehsan, "High step-up Z-source DC–DC converter with coupled inductors and switched capacitor cell," IET Power Electronics, vol. 8, no. 1, pp. 1394-1402, 2015.
23. F. Evran and M. T. Aydemir, "Z-source-based isolated high step-up converter," in IET Power Electronics, vol. 6, no. 1, pp. 117-124, Jan. 2013.
24. H. Shen, B. Zhang and D. Qiu, "Hybrid Z-Source Boost DC–DC Converters," in IEEE Transactions on Industrial Electronics, vol. 64, no. 1, pp. 310-319, Jan. 2017.
25. D. Vinnikov and I. Roasto, "Quasi-Z-Source-Based Isolated DC/DC Converters for Distributed Power Generation," in IEEE Transactions on Industrial Electronics, vol. 58, no. 1, pp. 192-201, Jan. 2011.
26. M. M. Haji-Esmaeili, E. Babaei and M. Sabahi, "High Step-Up Quasi-ZSource DC–DC Converter," in IEEE Transactions on Power Electronics, vol. 33, no. 12, pp. 10563-10571, Dec. 2018.
27. A. Ho, T. Chun and H. Kim, "Extended Boost Active-Switched-Capacitor/Switched-Inductor Quasi-Z-Source Inverters," in IEEE Transactions on Power Electronics, vol. 30, no. 10, pp. 5681-5690, Oct. 2015.
28. Y. P. Siwakoti, F. Z. Peng, F. Blaabjerg, P. C. Loh, and G. E. Town, "Impedance-Source Networks for Electric Power Conversion Part I: A Topological Review," IEEE Transactions on Power Electronics, vol. 30, no. 2, pp.699-716, 2015.

29. E. Babaei, E. S. Asl, M. H. Babayi, and S. Laali, "Developed embedded switched-Z-source inverter," IET on Power Electronics, vol. 9, no. 9, pp. 1828-1841, 2016.
30. W. Aian, F. Z. Peng, and H. Cha, "Trans-Z-source inverters," IEEE Transactions On Power Electronics, vol. 26, no.12, pp. 3453-3463, 2011.
31. H. Cha, F. Z. Peng, and D. W. Yoo, "Distributed impedance network (Z-network) DC/DC converter," IEEE Transactions On Power Electronics, vol. 25, no. 11, pp. 2722–2733, 2010.
32. A. Pressman, "Switching power supply design," Second edition, McGraw-Hill 1998.